Shock Waves (1996) 6: 161–166

Shock Waves

Drag measurements in a hypervelocity expansion tube

A.L. Smith, D.J. Mee

Department of Mechanical Engineering, The University of Queensland, Brisbane QLD 4072, Australia

Received 12 December 1995 / Accepted 29 April 1996

Abstract. A technique is described for the measurement of aerodynamic drag in a hypervelocity expansion tube in which the test flow period may be as short as 50 μs. The technique is an application of the stress wave force balance first proposed by Sanderson and Simmons (1991). The experiments were conducted in a test flow of partially dissociated Carbon Dioxide where the flow speed was in excess of 7 kms^{-1}. The validity of the technique is first demonstrated by comparing the forces measured on a range of sharp cones with those expected theoretically. Agreement to within 10% is achieved. Two re-entry type heat shield geometries were then tested with the experimental drag forces being compared with a Modified-Newtonian prediction. In both cases agreement to within 11% was obtained.

Key words: Drag measurement, Carbon Dioxide, Expansion tubes, Deconvolution, Hypervelocity, Re-entry vehicles

1 Introduction

Since the early 1960's experiments in hypervelocity flows have been conducted using shock tunnels. Shock tunnels are useful for conducting experiments for aerodynamics and propulsion purposes, at speeds up to Earth orbital velocities. However shock tunnels are limited in the range of stagnation enthalpies and test velocities that may be produced.

Free piston driven expansion tubes offer a wider range of stagnation enthalpies and test flow velocities and are therefore particularly useful in producing flows that are representative of re-entry at near orbital velocities.

The impulsive nature of both shock tunnels and expansion tube facilities restricts the steady test flow period that is produced. These may be as short as 1 ms for shock tunnels and 50 μs for expansion tubes. Consequently, traditional force measurement techniques cannot be employed as there is insufficient time for the model and its support to reach static equilibrium.

Correspondence to: D.J. Mee

Although a number of techniques have been proposed for the measurement of aerodynamic forces in short duration test flows, the most successful has been the stress wave force balance. This technique has been developed over the last five years to allow force measurements to be obtained on a variety of models in the T4 free piston shock tunnel, where the test time is around 1 ms.

This paper addresses an application of this experimental technique to the measurement of drag force in a hypervelocity expansion tube, where the test time is approximately 50 μs. It is envisaged that this measurement technique will be useful in the study of aerobraking and aerocapture manoeuvres within a Martian atmosphere.

2 Experimental facility

The experiments were conducted in the X1 facility located at The University of Queensland (Ref. Neely et al. 1991). This facility was originally designed as a reflected shock tunnel but has been adapted to investigate the mating of a free piston driver with an expansion tube. The X1 facility is shown schematically in Fig. 1.

The free piston driver uses a 3.4 kg piston which is contained within the compression tube. The compression tube has an internal diameter of 100 mm and is 2.3 m in length. Both the shock and acceleration tubes have internal diameters of 37 mm and are 2.08 m and 2.94 m in length, respectively.

The facility was operated as a free piston driven expansion tube using Carbon Dioxide as the test gas. The test condition produced approximately 50 μs of steady test flow. The typical filling pressures and test flow conditions, along with their respective uncertainties, are listed in Table 1. Also included is a prediction of the test flow composition which was obtained from an equilibrium chemistry solver. This code obtains the equilibrium concentration of species by Gibbs free energy minimisation.

Ideally finite rate chemical kinetics would be used to calculate the test conditions. Neely and Morgan (1994) used air as the test gas in the present facility, operating as a super-orbital expansion tube, and argued that equilibrium chemistry could be used in the calculations. They showed that the

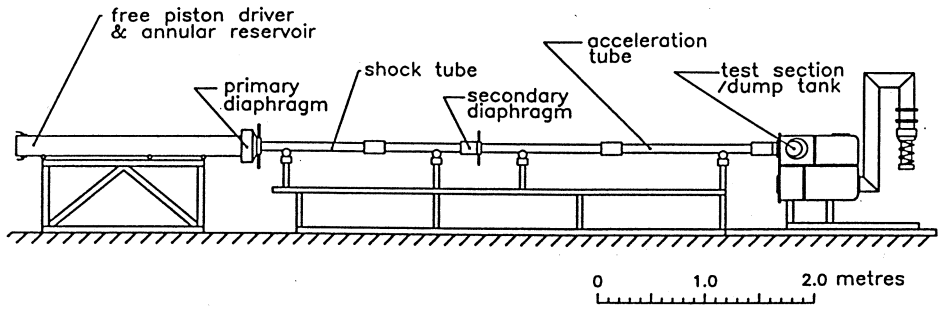

Fig. 1. Layout of the X1 facility

Table 1. Typical fill pressures and test conditions for the X1 facility

Operating Mode	Expansion Tube	
Driver gas	80% He	20% Ar
Test gas	CO_2	
Acceleration gas	He	
Fill Pressures		
Compression tube (kPa)	78 kPa He	17 kPa Ar
Shock Tube (kPa)	5 kPa	
Acceleration tube (Pa)	100 kPa	
Test Flow		
Shock velocity (ms^{-1})	7500	±2.0%
Test velocity (ms^{-1})	7500[1]	±2.0%
Static pressure (kPa)	15.6	±2.0%
Temperature (K)	2990[1]	±1.9%
Density (kgm^{-3})	0.0194[1]	±10.0%
Total Enthaply ($MJkg^{-1}$)	36.8[1]	±2.6%
Specific heat ratio	1.25[1]	±0.2%
Pitot pressure (kPa)	1230	±5.0%
Unit Reynolds number (m^{-1})	1.8×10^{6}	±10.4%
Mach number	7.4[1]	±4.3%
Test Flow Composition[2]		
Molecular Oxygen (O_2)	0.189	
Atomic Oxygen (O)	0.620×10^{-1}	
Carbon Dioxide (CO_2)	0.310	
Carbon Moxide (CO)	0.439	
Atomic Carbon (C)	0.192×10^{-10}	

[1] Quantity obtained from equilibrium chemistry solver.
[2] Expressed as a mass fraction.

high enthalpy flow conditions produced in the test section can only be achieved if the energy absorbed in dissociating the test gas, as it is processed by the primary shock, is at least partly restored through recombination in the unsteady expansion process. This was done by comparing the conditions calculated assuming equilibrium chemistry with those calculated assuming frozen chemistry, the latter producing unrealistically low pressures and temperatures. Similar calculations using equilibrium and frozen flow were performed for the present conditions with Carbon Dioxide as the test gas. The agreement found between predicted and measured Pitot and static pressure at the exit of the acceleration tube for the equilibrium chemistry case suggest that the equilibrium calculations are adequate for the present experiment.

The facility is instrumented with ionisation gauges and piezoelectric pressure transducers mounted along the walls of both the shock and acceleration tubes. These allow measurement of the shock speed and static wall pressure in both the shock and acceleration tubes. A piezoelectric pressure transducer was also used for measurements of the centreline Pitot pressure at the exit of the acceleration tube.

3 Force measurement technique

The force measurement technique presented here is based upon a scaled down version of a prototype stress wave force balance, originally designed by Sanderson and Simmons (1991). The stress wave force balance design has since been extended by Tuttle et al. (1995) and Porter et al. (1994) such that the technique is capable of resolving forces on a variety of model configurations, even those producing thrust, Paull et al. (1995). All these experiments were conducted in the T4 free piston shock tunnel, located at The University of Queensland. The most significant difference between the original stress wave force balance and the design presented here is the time in which forces are able to be resolved.

The stress wave force balance involves connecting the model to an elastic stress bar and suspending the arrangement in the test flow so that there is no restriction to movement in the flow direction (see Fig. 2). With the sudden arrival of the test flow a drag force is exerted on the model causing stress waves to propagate and reflect within the model and the stress bar. These stress waves are measured using strain gauges mounted on the stress bar. The dynamic behaviour of the system can be modelled as a linear system described by the convolution integral,

$$y(t) = \int_0^t g(t-\tau)u(\tau)d\tau \qquad (1)$$

where $u(t)$ is the input to the system (the drag force time history), $y(t)$ is the resulting output (the strain in the stress bar) and $g(t)$ is the unit inpulse response function. In experiments, the unknown drag on the model is determined from the measured output strain signal and the impulse response function. Thus, the problem is an inverse one and the drag may be found using a numerical deconvolution procedure. This procedure has been developed in more detail by Tuttle et al. (1995).

4 Force balance development

The application of the stress wave force balance presented in this paper scales directly from previous work conducted in T4 in that the number of reflections of stress waves within the models during the test times are similar and the

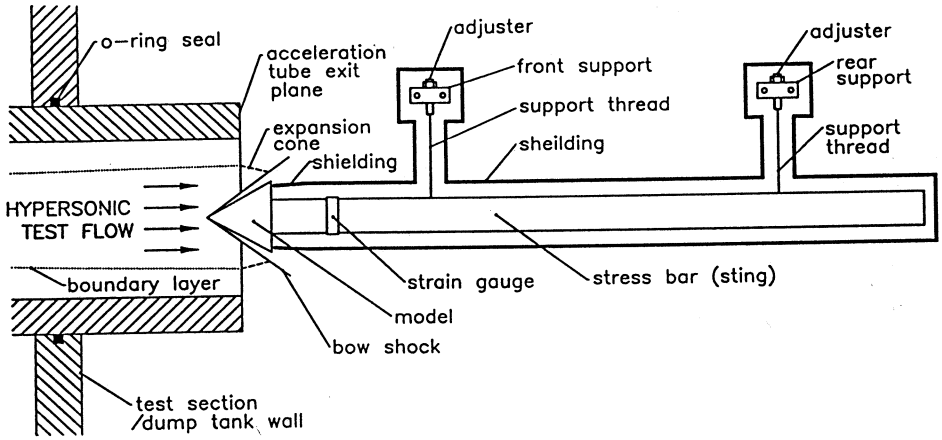

Fig. 2. A schematic representation of the X1 force balance

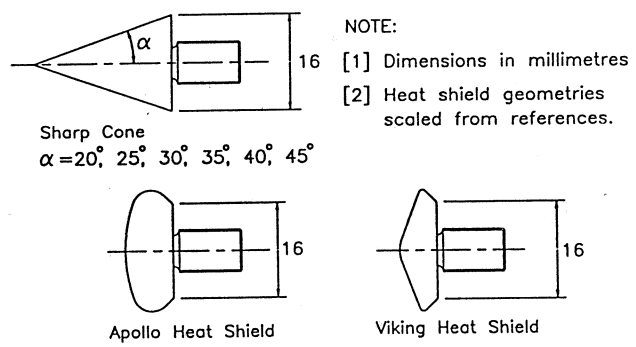

Fig. 3. The model geometries used in the X1 facility

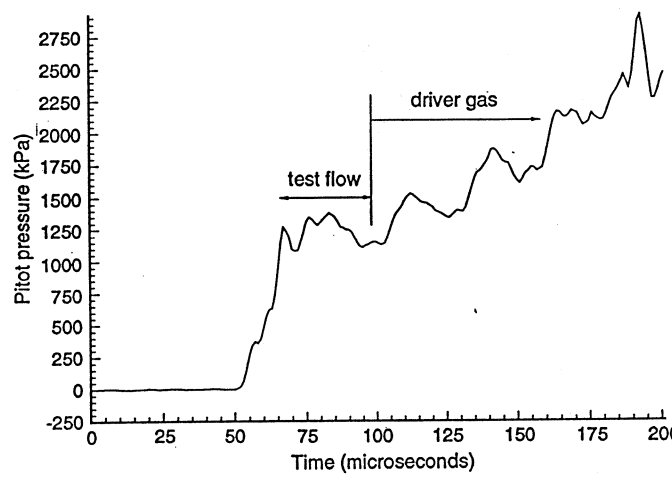

Fig. 4. A typical Pitot pressure time history measured in the X1 facility

impedance matching between the models and stress bars are similar.

The performance of the proposed design was tested using dynamic finite element modelling of the arrangement to calculate the response of the balance to expected tunnel drag time histories. Deconvolution of this output with the impulse responses (also calculated using dynamic finite element modelling) indicated that, in the absense of noise, the applied load could be recovered to within 1%. When processing shock tunnel signals, work by Sanderson and Simmons (1991) and Tuttle et al. (1995) demonstrates that forces can be measured to within 10%.

The force balance was designed to mount within the test section of the X1 facility and to support a small model within the test flow. Predictions of the test core, based upon the development of the boundary layer in the acceleration tube, indicated that the maximum model size was approximately 20 mm in diameter. The expansion cone produced by the expanding test gas (refer to Fig. 2) constrained the model geometry such that oblique bow shock reflections from the expansion cone would not impinge on the model. This was a particular concern for conical models.

Based on the above geometrical constraints, eight different models were manufactured: a series of sharp cones ranging in angle from 20° to 45° in increments of 5°, an Apollo heat shield (Ref. Park 1990) and a Viking heat shield (Ref. Miller 1975) (refer to Fig. 3). All of the models were made from 4140 Steel which was sufficiently robust to withstand the severity of the test conditions. The models were threaded into the stress bar.

The brass stress bar of 8 mm outside diameter, 7 mm inside diameter and 550 mm length, was instrumented with Kulite ULP-120-160 semi-conductor strain gauges. The strain gauges were mounted in a half bridge (bending compensation arrangement), approximately 60 mm remote from the threaded conection to the model. This formed the basis of the force balance onto which all the different models could be attached. Brass was chosen as the stress bar material because it has a relatively low elastic wave speed (3560 ms^{-1}). This serves to increase the period before stress waves reflected from the downstream end return to the gauge location. The instrumented stress bar was then suspended in a rigid shielding and aligned so that a small gap remained between the model and the shielding (refer to Fig. 2).

A DC strain gauge amplifier, with a response time of approximately 1 μs, was coupled to a transient data recorded with a 1 MHz sample rate. This arrangement provided a sufficiently fast response that approximately 50 samples could be taken during the test time. This was found to be adequate for deconvolution of the drag force on the model.

Note that the arrangement of the stress bar and shielding at the base of the model will influence the base pressure. The balance geometry was designed to minimize the pressure acting on the base of the models by minimizing the gap between the model and the shielding. A finite gap is necessary in order to allow the model to be free to move under the

influence of the aerodynamic drag. For the present models it is estimated that this gap needs to be at least 0.03 mm to ensure that the model does not come into contact with the buffer during the test time. For practical purposes the gap distace was approximately 0.5 mm.

The dynamic responses of the eight different model/stress bar arrangments were analysed using the finite element package MSC/NASTRAN. This enabled unit step responses to be obtained for a uniformly distributed pressure loading on the models. The unit step responses were then used to obtain the unit impulse response functions which were later used in the deconvolution of the measured strain time histories.

5 Experimental results

Experiments were conducted in two stages. The first stage involved demonstrating that the force balance could be used to obtain drag measurements on simple models by comparing the results with theoretical predictions. The second stage consisted of drag measurements on two typical re-entry type vehicle configurations in a hypervelocity flow and comparisons with a simple Modified-Newtonian prediction.

5.1 Verification of force balance

At the chosen test condition, the X1 facility produced a steady test flow for a period of approximately 50 μs. This is illustrated in Fig. 4 by a typical centre-line Pitot pressure time history. The Pitot pressure time history is characterised by the initial rise in pressure due to the acceleration gas, followed by the arrival of the test gas. Expansion waves from the driver then cause the Pitot pressure to rise rapidly, indicating the end of the test flow and the arrival of the driver gas.

Drag measurements were obtained for the conical models through deconvolution of the measured strain time histories, as described in Sect. 3. The deconvolved drag measurements were then compared directly to a theoretical drag prediction. The prediction was based upon the inviscid Taylor-Maccoll (1932) theory for an attached conical shock with frozen chemistry.

As a check on the suitability of the prediction, a comparison of frozen and equilibrium chemistry was made. For the 30° cone model, predictions of the surface pressure were made using a finite volume, Euler solver with Riemann flux differencing. The predictions were made on an axisymetric model using frozen and equilibrium chemistry routines. The results obtained differed from one another by only 0.5% and by 1% from the Taylor-Maccoll prediction.

For all cases the bow shock produced was fully attached and the conditions behind the shock were used to estimate the effect of skin friction. An estimate of the pressure acting in the base region was made by assuming that the pressure in that region starts from the inital test section pressure and rises with time as gas leaks through the gap (Refer to Fig. 2). This build up of pressure is estimated by assuming choked flow from the conditions behind the conical shock on the model. The results from these calculations indicated that the combined effect of skin friction on the model and pressure

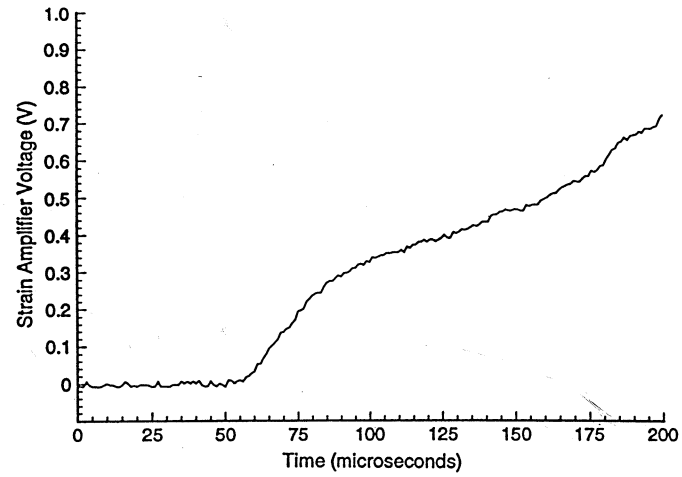

Fig. 5. Raw strain gauge amplifer output for the drag on the 30° cone model [CO_2 at M=7.4]

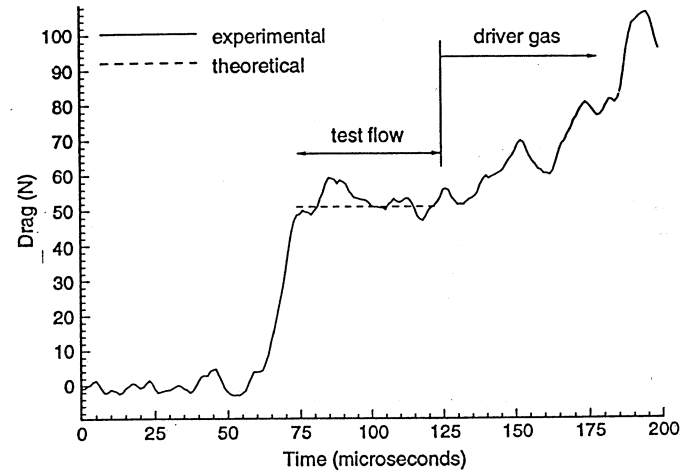

Fig. 6. A comparison between the measured and predicted drag force on the 30° cone model [CO_2 at M=7.4]

acting in the base region was less than 2% of the net drag on the model during the period of the test flow.

A raw strain time history along with the corresponding deconvolved drag time history appears as Figs. 5 and 6. This signal was obtained from the 30° cone model. The predicted drag force level is also shown for comparison purposes in Fig. 6.

Figures 4 and 6 indicate that the deconvolved drag has a similar time history to the measured Pitot pressure, in that a steady drag level is measured during the period of the test flow. Note that size restrictions in the test section prevented Pitot pressure and drag measurements being obtained simultaneously. Thus zero on the time scale is arbitary.

Agreement between predicted and experimental drag levels was found to be within 10% for repeated tests on all the conical models. The difference was attributed primarily to uncertainties in the test flow conditions which corresponded to a 12% uncertainty in the measured drag coefficient. The comparison between experimental and theoretical drag coefficients for the range of cones tested is presented in Fig. 7. The error bars correspond to the level of uncertainty in the theoretical results, based on uncertainty in flow conditions.

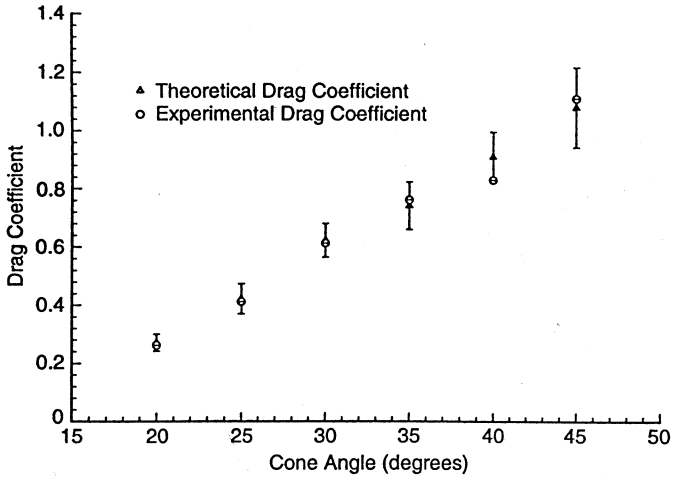

Fig. 7. A comparison of the experimental and theoretical drag coefficients on increasing cone angles [CO_2 at M=7.4]

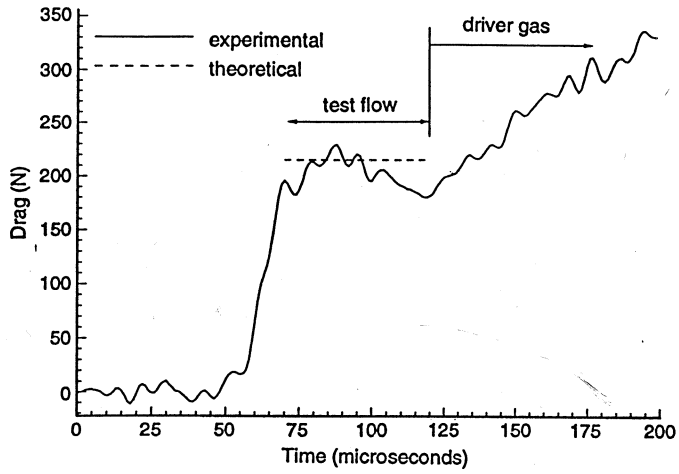

Fig. 8. The measured and predicted drag force on the Apollo heat shield model [CO_2 at M=7.4]

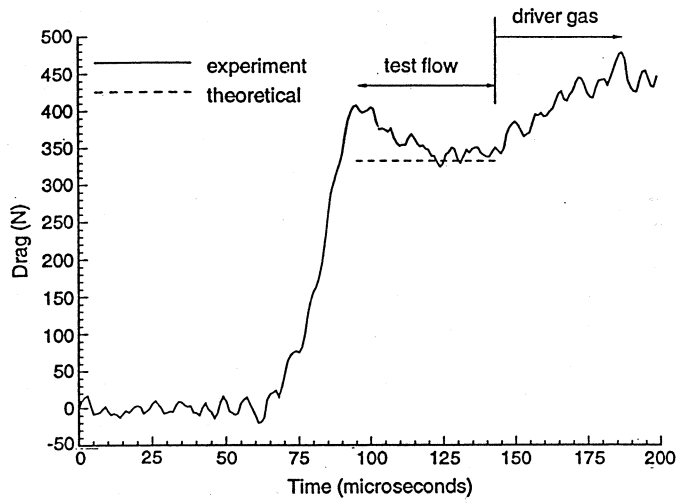

Fig. 9. The measured and predicted drag force on the Viking heat shield model [CO_2 at M=7.4]

The results from the experiments on the conical models indicate that the present balance is capable of measuring the drag of models in the short duration flows. The accuracy of the measured drag is estimated to be ± 10% for a 95% confidence interval. In the next section the balance is used to investigate the drag on re-entry models in the expansion tube flow.

5.2 Drag force measurements on re-entry heat shields

The force balance was used to obtain drag measurements on the Apollo and Viking heat shield models, as depicted in Fig. 2. Figures 8 and 9 illustrate typical deconvolved drag measurements for the Apollo and Viking heat shield models respectively, plotted for the duration of the test flow. The inital overshoot in the measured drag time history has been attributed to the time associated with the formation of the bow shock over the blunt model. Davies (1964) reports that the formation of the bow shock wave over a Pitot probe resulted in an overshoot in the pressure/force time history. An overshoot was also observed in the drag time histories for some of the conical models. In general, an increased cone angle resulted in a larger initial overshoot in the drag. Figures 8 and 9 again indicate that the deconvolved drag time history follows the Pitot pressure time history.

Theoretical predictions for the drag on these models were made using the finite element meshes of the models described in Section 4 and a Modified-Newtonian flow solver with frozen chemistry. An example of the finite element meshes for the Apollo heat shield used is presented in Fig. 10. The effect of skin friction and pressure in the base region was less significant for the re-entry models than the conical models. This is due to the bluntness of the models. Therefore this did not represent a significant uncertainty in obtaining drag force predictions. The predicted force levels are shown in Fig. 8 and 9.

Repeat shots on both models were used to obtain drag coefficients. This showed that agreement between experimental and predicted drag levels was to within 11%. The measured and predicted drag levels for all tests were averaged and normalised for the nominal test conditions and are presented in Table 2.

The agreement is to within the uncertainty of test conditions produced by the X1 facility and it is interesting that the Modified-Newtonian calculations give reasonable drag levels using a simple frozen chemistry model of the flow. This is not surprising given that, for the present models and flow conditions, the shock shape should be quite similar to the body shape.

6 Conclusion

An application of the force measurement technique has been developed for use in a free piston driven expansion tube. Pre-

Table 2. Average measured and predicted drag coefficients for typical re-entry heat shields [CO_2 at M=7.4]

Model	$C_{D(measured)}$	$C_{D(predicted)}$
Apollo Heat Shield	1.56	1.60
Viking Heat Shield	1.81	1.65

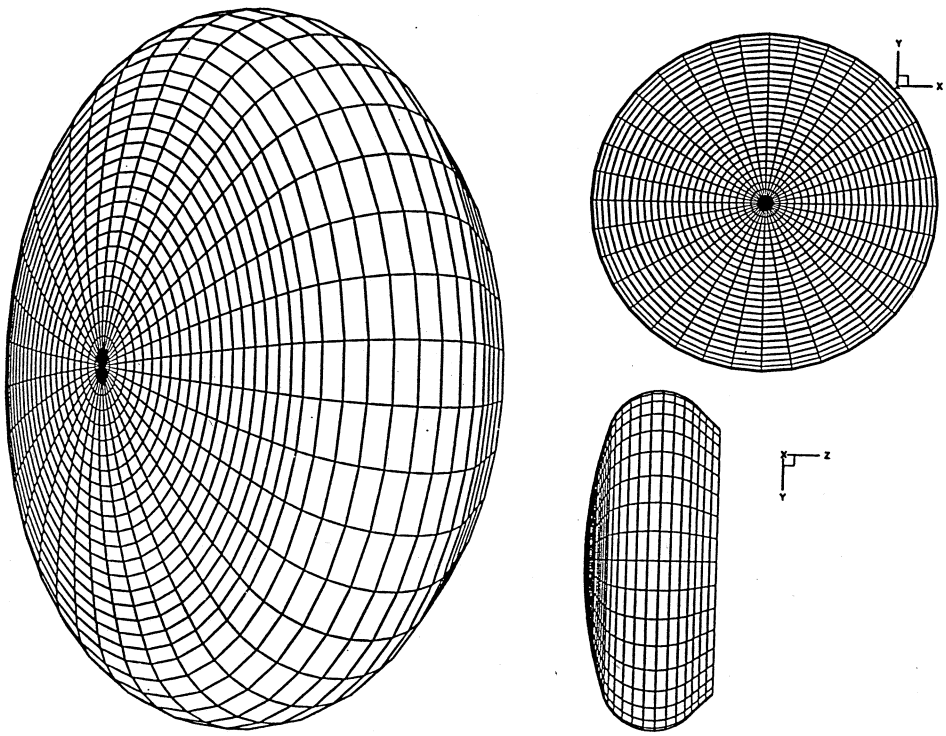

Fig. 10. The finite element mesh of the Apollo heat shield used in conjuction with the Modified-Newtonian flow solver

liminary tests were used to verify the response of the force balance to the short duration test flows that are typical of expansion tubes. The force balance was then used to obtain drag measurements on two re-entry type vehicles shapes, in partially dissociated Carbon Dioxide test flows. In general, agreement between experimental and predicted drag levels was found to be within 11%.

The successful measurement of drag forces in the X1 facility extends the usefulness of short duration hypervelocity facilities, especially in the area of aerobraking and aerocapture studies. This is envisaged to be important for the development of interplanetary flight vehicles.

Acknowledgements. The authors gratefully acknowledge the financial support of the Australian Research Council under grant A8941305. Thanks also go to I. Johnston and K. Austin, both of The University of Queensland, Department of Mechanical Engineering, for their assistance in the Euler and Modified-Newtonian calcualtions respectively.

References

Sanderson SR, Simmons JM (1991) Drag balance for hypervelocity impulse facilities. AIAA Journal 29(12): 2185–2191

Neely AJ, Stalker RJ, Paull A (1991) High enthalpy, hypervelocity flows of air and argon in an expansion tube. The Aeronautical Journal, 175–186, June/July

Neely AJ, Morgan RG (1994) The Superorbital Expansion Tube concept, experiment and analysis. The Aeronautical Journal, 97–105, March

Tuttle SL, Mee DJ, Simmons JM (1995) Drag measurements at Mach 5 using a stress wave force balance. Experiments in Fluids 19(5): 336–341

Porter LM, Paull A, Mee DJ, Simmons JM (1994) Shock tunnel measurements of hypervelocity blunted cone drag. AIAA 32(12): 2476–2477

Paull A, Stalker RJ, Mee DJ (1995) Scramjet thrust measurement in a shock tunnel. The Aeronautical Jounal, 161–163, May

Park C (1990) Nonequlibrium Hypersonic aerothermodynamics. John Wiley and Sons, New York

Miller CG (1975) Shock shapes on blunt bodies in hypersonic-hypervelocity helium, air and CO2 flows, and calibration results in Langley 6-inch expansion tube. NASA TN D-7800

Taylor GI, Maccoll JW (1932) The air pressure on a cone moving at high speed. Proc. Royal Society (London) Series A 139: 278–297

Davies L (1964) Bow-shock establishment and stagnation-point pressure measurements for a blunt-nosed body at supersonic speeds. NPL Aero Report 1098